Korean J. Chem. Eng., 38(9), 1791-1796 (2021)
DOI: 10.1007/s11814-021-0797-1

pISSN: 0256-1115
eISSN: 1975-7220

Solid-state reaction between MoS_2 and MoO_3 in a fluidized bed reactor

Jae-Rang Lee*, Yong-Ha Kim,†, and Yong Sun Won**,†**

*Climate Change Research Division, Korea Institute of Energy Research, 152 Gajeong-ro, Yuseong-gu, Daejeon 34129, Korea
**Department of Chemical Engineering, Pukyong National University, 45 Yongso-ro, Nam-gu, Busan 48513, Korea
(*Received 30 November 2020 • Revised 2 March 2021 • Accepted 4 April 2021*)

Abstract−MoO_2 was produced by mixing MoS_2 and MoO_3 via a solid-state reaction in a fluidized bed reactor. The basic fluidization data were acquired by monitoring the minimum fluidization velocity of MoS_2 and MoO_3. The conversion rate of MoS_2 and MoO_3 to MoO_2 was derived based on the solid-state reactions carried out for 1 h at various stoichiometric ratios. This study confirmed that the optimal stoichiometric ratio of MoS_2 and MoO_3 was 1.0 : 6. The conversion rate at the optimum stoichiometric ratio was studied by varying the reaction temperature. A conversion rate of 99% was achieved when the reaction temperature and superficial gas velocity were 973 K and 0.3 m/s, respectively. Detailed analysis of the final product after the solid-state reaction was by scanning electron microscopy (SEM), transmission electron microscopy (TEM), energy-dispersive spectrometry (EDS) and X-ray diffraction (XRD), to determine the shape, structure, and diffraction patterns.

Keywords: Fluidized Bed Reactor, Fluidization, Solid-state Reaction, Minimum Fluidization Velocity, Conversion Rate

INTRODUCTION

Fluidized bed technology finds a variety of applications in the environmental, chemical, and steelmaking industries. Among them, a technology for obtaining the desired materials using a fluidized bed has attracted the attention of researchers, especially in the steelmaking industry [1-3].

Solid state reactions of small amounts of particles in a laboratory-scale horizontal furnace show ideal results. However, the limitations of the horizontal furnace in the application on the actual industrial scale are evident. Fluidized bed technology has been used from the past to the present for mass production [4-7]. Fluidized bed technology is capable of high efficiency gas-solid contact and high heat and mass transfer. In addition, it is used as basic data for designing an industrial-scale fluidized bed reactor based on laboratory-scale fluidized bed reactor experiment results [8,9]. Developed nations are thus making great efforts to utilize fluidized bed technology for producing high-quality value-added metals, contributing to their technical advances [10,11].

Molybdenum has high melting point and superior thermal conductivity, and strong corrosion resistance. It is used in high-temperature materials such as missiles, aircraft, and filaments based on these advantages. Mo, MoO_2, and MoO_3 are used depending on the property of the material that is required in industry [12,13]. Since the early 1960s, attempts have been made to produce MoO_2 (molybdenum dioxide) from the molybdenum chemical family. One such method is the mixed reaction of MoO_3 (molybdenum trioxide) and MoS_2 (molybdenum disulfide). The solid-state reaction of MoS_2 and MoO_3 can be expressed as follows [14]:

$$MoS_2+6MoO_3 \rightarrow 7MoO_2+2SO_2$$

The reduction of MoO_3 by hydrogen (H_2) is another possible method for obtaining MoO_2, but H_2 is expensive and secondary pollutants are generated during H_2 production [15,16]. Thus up to now, various methods for producing MoO_2 in an efficient manner have been investigated [17], with research on the solid-state reaction of MoS_2 and MoO_3 also underway [18]. Anyhow, it is necessary to develop new metal production techniques via the mixed reaction of various solids in a fluidized bed, and detailed analysis of research results will contribute to the study of fluidization and steelmaking [19,20].

In the present study, MoO_2 was produced by the mixed reaction of MoS_2 and MoO_3 in a fluidized bed via a solid-state reaction. The fluidization characteristics were investigated based on the minimum fluidization velocity of MoS_2 and MoO_3. The reaction extent for obtaining MoO_2 by the solid-state reaction at an optimal stoichiometric ratio was also verified. Furthermore, the structural, constitutional and morphological features of the final product were analyzed by scanning electron microscopy (SEM), transmission electron microscopy (TEM), energy-dispersive spectrometry (EDS) mapping, and X-ray diffraction (XRD).

EXPERIMENTAL

1. Materials

Table 1 lists the physical properties of MoS_2 and MoO_3 particles. The particle sizes of MoS_2 and MoO_3 were examined using a particle size distribution analyzer (TSI, USA). The particle density and bulk density were calculated based on ISO 12154:2014 [21], and constitutional analysis was performed using inductively coupled plasma-optical emission spectrometry (ICP-OES, Perkin Elmer Co., USA). The MoS_2 and MoO_3 particles were included in Geldart

†To whom correspondence should be addressed.
E-mail: yhkim@pknu.ac.kr, yswon@pknu.ac.kr

Table 1. Physical properties of MoS_2 and MoO_3 particles

	MoS_2	MoO_3
Mean particle size [μm]	55	109
Particle density [kg/m^3]	3,900	4,086
Bulk density [kg/m^3]	1,151	1,746
Shape [-]	Board	Stick
Geldart group classification [-]	B	B

Table 2. Experimental conditions

Parameter	Value
Fluidizing gas [-]	Nitrogen
Superficial gas velocity [m/s]	Up to 0.45
Bed diameter [cm]	5
Reaction time [min]	60
Reaction temperature [K]	573 to 1,073

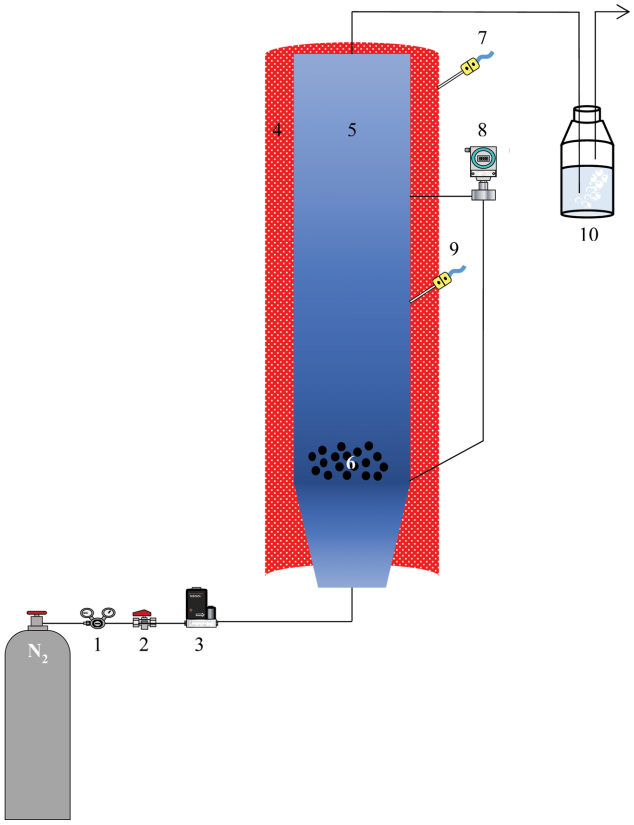

Fig. 1. Schematic of the experimental apparatus.

1. Regulator
2. Valve
3. Mass flow controller of N_2
4. Heating jacket
5. Fluidized bed reactor
6. Particles
7. Temperature sensor of heating jacket
8. Differential pressure transmitter
9. Temperature sensor of fluidized bed reactor
10. Beaker with water

group B, considering the particle size and density according to the Geldart classification [22-24].

2. Methods

Fig. 1 and Table 2 show the schematic and experimental conditions, respectively. For the fluidized bed reactor, a mesh-type distributor with an inner diameter of 50 mm and a height of 1,590 mm was installed. To measure the pressure drop ports were installed above the distributor and at the maximum bubbling height of the particles. The pressure drop was recorded every 30 sec using a pressure drop sensor (Differential Pressure Transmitter, Rosemount Inc., USA). The stabilization time for the fluidization process was set to 30 min, and nitrogen (N_2) was used as the fluidizing gas. The mixture of MoS_2 and MoO_3 was placed in the fluidized bed at the desired reaction temperature after adjusting the stoichiometric ratio of MoS_2 and MoO_3.

The temperature of the heating jacket is controlled with a thermal couple inside the fluidized bed reactor. The power that is supplied to the heating jacket is decreased when the internal temperature is increased due to the solid state reaction in the exothermic reaction. Therefore, it was maintained constant at the desired reactor temperature. The solid state reaction time was set to 60 min to determine the conversion rate.

After the completion of the solid-state reaction, the product was cooled to room temperature and analyzed by SEM (Hitachi, Japan), TEM (FEI Co., Netherlands), EDS (FEI Co., Netherlands), and XRD (Rigaku, Japan). The SO_2 generated from the solid-state reaction was captured using a beaker filled with water.

3. Reaction Kinetics

Solid-state reactions are complex, and the underlying mechanisms are difficult to understand. Reactions between gases and solids are of great importance in many process metallurgical operations. Generally, the most common gas-solid reaction practices are: roasting of metal sulfides to metal oxides, reduction of metal oxides to metals and decomposition of metal compounds to metal oxides. The simplest way to describe a gas-solid reaction system is to imagine a single solid sphere which is placed in contact with a reacting gas stream. Eq. (1) is a representative equation for gas-solid reactions [25].

$$A(g)+B(s)=C(g)+D(s) \quad (1)$$

Representative gas and solid reactions are shown in Eq. (2).

$$gas+particle=product \quad (2)$$

The chemical reaction of gas and solid comprises reaction kinetics.

4. Fluidization

Fluidized bed is a system that facilitates gas-solid contact and reaction. Fluidization is defined as when gas and solid contact and behave fluid like. In a gas-solid system, the amount of solids is fixed and the properties of the gas may change according to temperature. The relationship between gas velocity and pressure drop can be understood based on Darcy's law [26-28]. The gas density decreases as the temperature is raised. The decrease in gas density that acts in the fluidized bed reactor leads to a decrease in the pressure drop. The correlation between gas velocity and pressure drop based on Darcy's law is as shown in Eq. (3).

$$\frac{V}{A}=\mu=\frac{k\cdot\Delta h_w}{h_b} \quad (3)$$

where, V is the volumetric flow rate of the fluid passing through a porous medium, A is bed cross-section area, μ is the fluid density, k is a constant depending on the physical properties of the particle bed and on the fluid (permeability), Δh_w is the pressure drop across the bed, h_b is the height of the bed.

RESULTS AND DISCUSSION

1. Minimum Fluidization Velocity

The minimum fluidization velocity according to the stoichiometric ratio of MoS_2 and MoO_3 is as shown in Fig. 2. The stoichiometric ratios of MoS_2 and MoO_3, which can be charged into a fluidized bed reactor and are applicable to the field, were set to 0.7 : 4.2, 0.8 : 4.8, 1.0 : 6, 1.2 : 7, and 1.3 : 7.8. The minimum fluidization velocities of 0.7 : 4.2 and 1.3 : 7.8 at 573 K were 0.35 and 0.4 m/s, respectively, and 0.07 and 0.2 m/s at 1,073 K, respectively. The amount of particles increases as the stoichiometric ratio of MoS_2 and MoO_3 increases, thereby showing a high minimum fluidization velocity. A minimum fluidization velocity was shown as the reaction temperature increased. Fluidization of particles in a

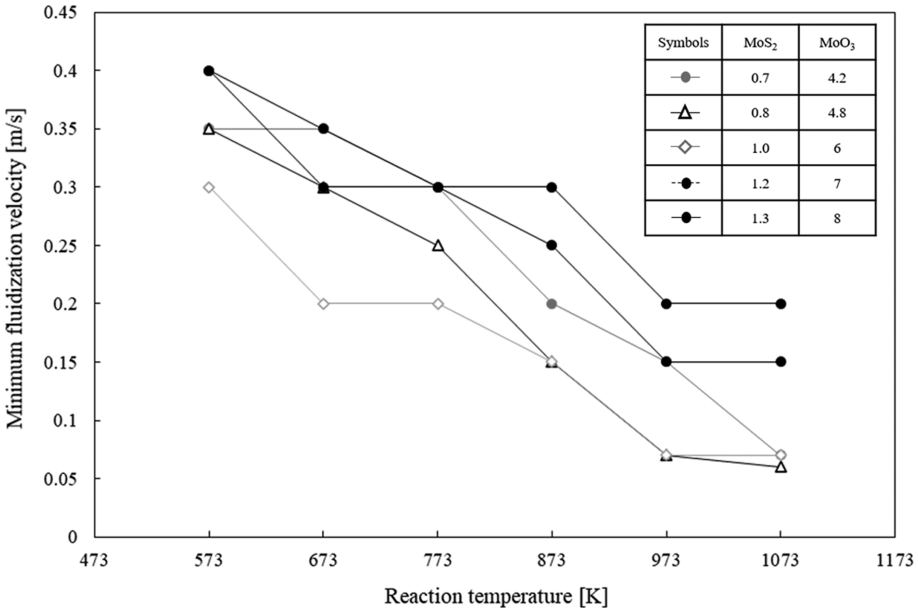

Fig. 2. Minimum fluidization velocity by temperature according to the stoichiometric ratio of MoS_2 and MoO_3.

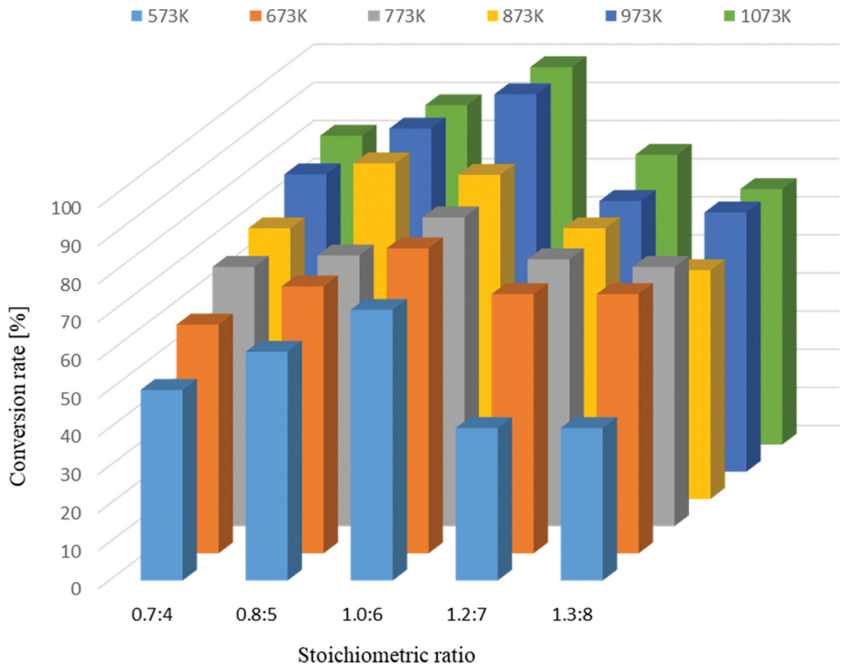

Fig. 3. Conversion rate according to temperature.

fluidized bed is achieved by a gas-solid reaction, with the reaction temperature playing an important role in this process.

2. Conversion Rate

The conversion rates of MoS_2 and MoO_3 according to the stoichiometric ratio are as shown in Fig. 3. The stoichiometric ratios of MoS_2 and MoO_3 of 0.7 : 4.2, 0.8 : 4.8, 1.0 : 6, 1.2 : 7, 1.3 : 7.8 were set as the variables. The conversion rates of 1.3 : 8 and 1.0 : 6 at 573 K were 40 and 71%. The conversion rates of 1.3 : 8 and 1.0 : 6 at 973 K were 68 and 99%. Both MoS_2 and MoO_3 based on stoichiometric ratio were 99% at 973 and 1,073 K of 1.0 : 6, so raising the reaction temperature further was meaningless. The contact rate of gas-solid increased as the reaction temperature increased, thereby raising the conversion rate. However, the optimal stoichiometric ratio and limit reaction temperature of MoS_2 and MoO_3 were investigated.

3. SEM

The SEM images of the experimental results were examined with a stoichiometric ratio of 1.0 : 6 of MoS_2 and MoO_3 with good conversion rates at a reaction time of 60 minutes and a reaction

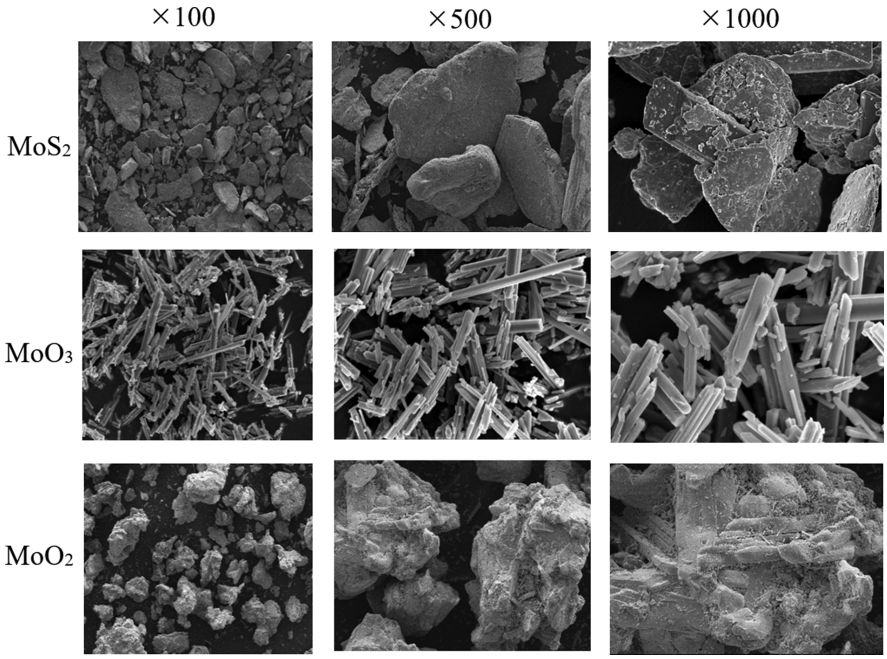

Fig. 4. SEM images of MoS_2, MoO_3 and MoO_2 after the solid-state reaction.

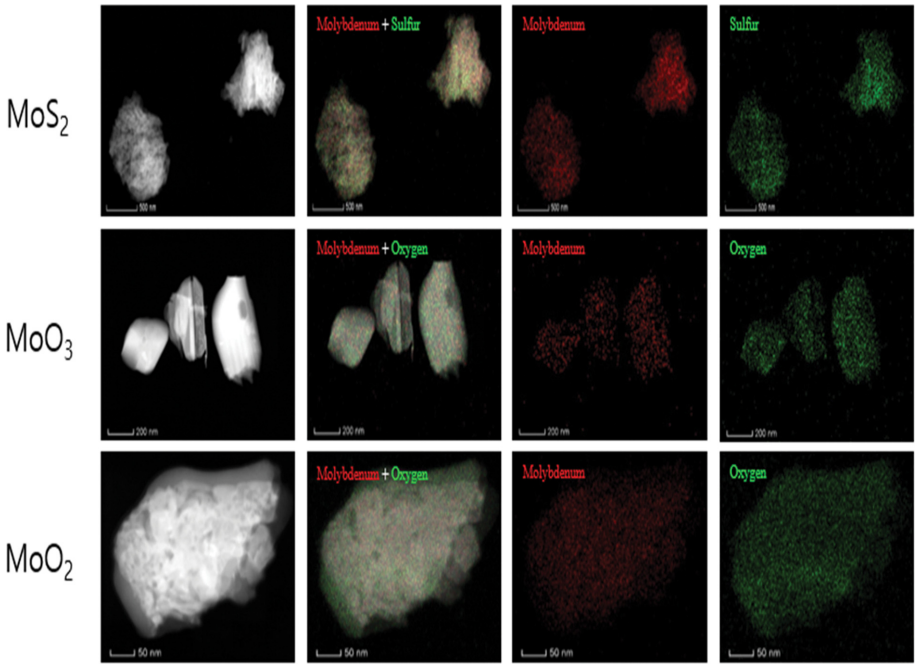

Fig. 5. TEM and EDS mapping images of MoS_2, MoO_3 and MoO_2 after the solid-state reaction.

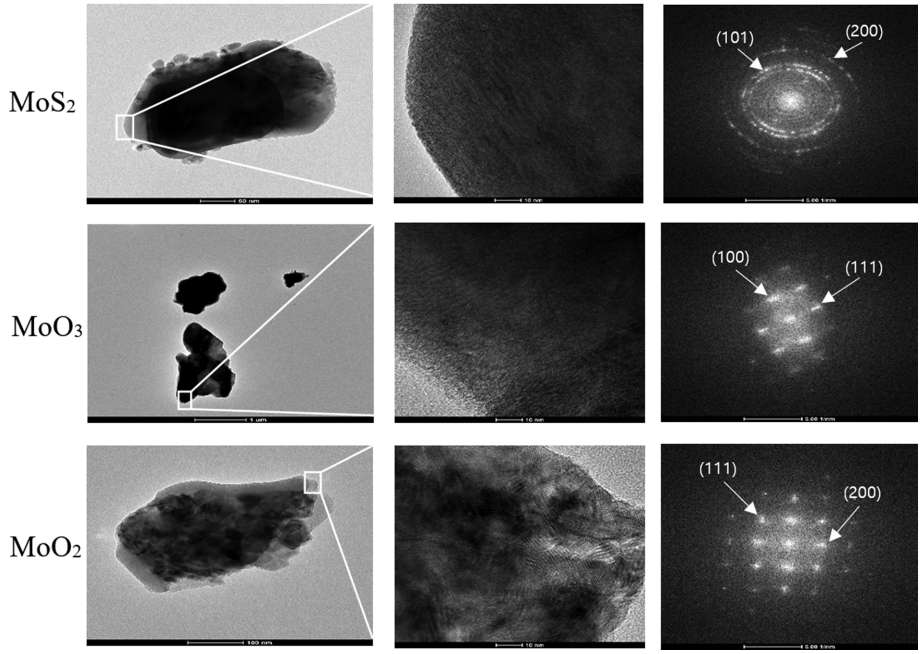

Fig. 6. TEM images and SAED patterns of MoS_2, MoO_3 and MoO_2 after the solid-state reaction.

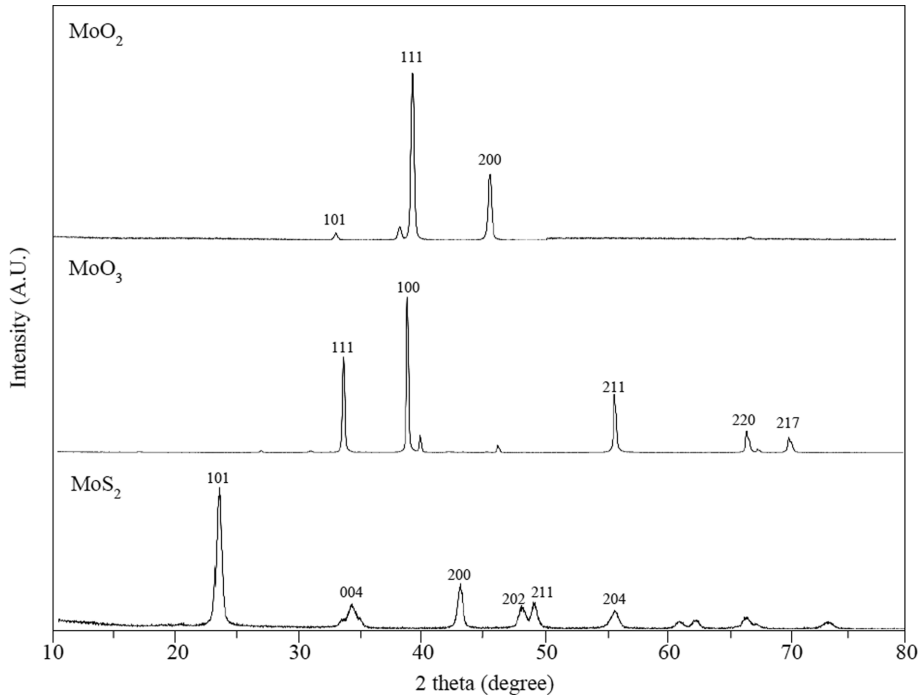

Fig. 7. XRD patterns of MoS_2, MoO_3 and MoO_2 after the solid-state reaction.

temperature of 973 K. Fig. 4 shows the SEM images of MoS_2 and MoO_3 particles, and the image of MoO_2 particle after the solid-state reaction. The MoS_2 were board-like, while and MoO_3 were stick-shaped. The MoO_2 particle showed a non-spherical shape after the solid-state reaction, of which structural and morphological changes seemed to be affected by initial particle shapes.

4. TEM, EDS Mapping, and XRD Analysis

Fig. 5 shows the TEM-EDS mapping results for MoO_2 produced by the solid-state reaction of MoS_2 and MoO_3. There was no residual sulfur in the MoO_2 output and only Mo and oxygen were detected. Fig. 6 shows the TEM images of particles and the selected area electron diffraction (SAED) pattern of the product, and Fig. 7 shows the XRD patterns for particles and product.

The XRD patterns confirmed that the [101] and [200] peak intensities were the highest for MoS_2, whereas for MoO_3 the [111] and [100] peak intensities were the highest. After the solid-state

reaction, the [111] and [200] peak intensities became the highest for MoO_2. The results of TEM-EDS mapping showed that the main components of MoO_2 were Mo and oxygen. The SAED patterns were examined and the results were consistent with the XRD patterns. The [111] and [200] peak intensities for MoS_2 and MoO_3 were consistent with those observed for MoO_2.

CONCLUSION

A fluidized bed reactor was used to produce MoO_2 via the solid-state reaction of MoS_2 and MoO_3. The fluidization characteristics of MoS_2 and MoO_3 were first studied, and subsequently, the optimal stoichiometric ratio for MoS_2 and MoO_3 was identified. A variable was established in the stoichiometric ratio of MoS_2 and MoO_3, thereby showing a lower minimum fluidization velocity as the reaction temperature was increased. The optimum experimental conditions were found to be the stoichiometric ratio of 1.0 : 6 of MoS_2 and MoO_3, which has the most superior conversion rate with MoO_2, at a reaction time of 60 minutes and a reaction temperature of 973 K.

Under these conditions, the highest conversion rate to MoO_2 was achieved. SEM analysis revealed that the output MoO_2 obtained from the solid-state reaction of MoS_2 and MoO_3 consisted of non-spherical particles unlike the reaction inputs. TEM analysis conducted on the particles indicated that the [111] and [200] peak intensities for MoS_2 and MoO_3 were consistent with those observed for MoO_2.

ACKNOWLEDGEMENT

This work was supported by the Korean Institute of Energy Technology Evaluation and Planning (KETEP) and the Ministry of Trade, Industry & Energy (MOTIE) of the Republic of Korea (No. 20172010106310) and the BB21 + Project in 2021.

REFERENCES

1. J. R. Lee, K. S. Lee, Y. O. Park and K. Y. Lee, *Chem. Eng. J.*, **380**, 122454 (2020).
2. J. R. Lee, N. Hasolli, K. S. Lee, K. Y. Lee and Y. O. Park, *Korean J. Chem. Eng.*, **36**, 1548 (2019).
3. J. R. Lee, K. S. Lee, N. Hasolli, Y. O. Park, K. Y. Lee and Y. H. Kim, *Chem. Eng. Process.*, **149**, 107856 (2020).
4. F. Podczeck, *Powder Technol.*, **93**, 47 (1997).
5. M. Cho, *ISIJ International*, **42**, 33 (2002).
6. J. R. Lee and Y. H. Kim, *Chem. Eng. Res. Des.*, **168**, 193 (2021).
7. X. Zhang, Y. Han, Y. Sun and Y. Li, *Powder Technol.*, **352**, 16 (2019).
8. Y. Jin, H. Lu, X. Guo and X. Gong, *Powder Technol.*, **376**, 468 (2020).
9. W. Ge, Q. Chang, C. Li and J. Wang, *Chem. Eng. Sci.*, **198**, 198 (2019).
10. G. H. Zhang, J. J. Li, L. Wang and K. C. Chou, *Int. J. Refract. Met. Hard Mater.*, **69**, 180 (2017).
11. B. Zhang, N. Kobayashi and Y. Itaya, *Powder Technol.*, **343**, 309 (2019).
12. G. S. Kim, Y. J. Lee, D. G. Kim and Y. D. Kim, *J. Alloys Compd.*, **454**, 327 (2008).
13. G. S. Kim, H. G. Kim, D. G. Kim, S. T. Oh, M. J. Suk and Y. D. Kim, *J. Alloys Compd.*, **469**, 401 (2009).
14. C. Raymond, U.S. Patent, 3,336,100 (1967).
15. K. Manukyan, D. Davtyan, J. Bossert and S. Kharatyan, *Chem. Eng. J.*, **168**, 925 (2011).
16. B. S. Kim, E. Y. Kim, H. S. Jeon, H. I. Lee and J. C. Lee, *Mater. Trans.*, **49**, 2147 (2008).
17. J. D. Lessard, L. N. Shekhter, D. G. Gribbin and L. F. McHugh, *JOM*, **65**, 1566 (2013).
18. L. Wang, C. Y. Bu, G. H. Zhang, T. Jiang and K. C. Chou, *JOM*, **68**, 1031 (2016).
19. H. K. Bizhaem and H. B. Tabrizi, *Powder Technol.*, **237**, 14 (2013).
20. D. Barletta and M. Poletto, *Powder Technol.*, **225**, 93 (2012).
21. J. R. Lee, N. Hasolli, S. M. Jeon, K. S. Lee, K. D. Kim, Y. H. Kim, K. Y. Lee and Y. O. Park, *Korean J. Chem. Eng.*, **35**, 2321 (2018).
22. N. Mostoufi, *Chem. Eng. Sci.*, **229**, 116029 (2021).
23. D. Geldart, *Powder Technol.*, **7**, 285 (1973).
24. L. Wei, Y. Lu, J. Zhu, G. Jiang, J. Hu and H. Teng, *Korean J. Chem. Eng.*, **35**, 2117 (2018).
25. H. Y. Lin, Y. W. Chen and C. Li, *Thermochim. Acta*, **400**, 61 (2003).
26. M. Ishida and C. Y. Wen, *AIChE J.*, **14**, 311 (1968).
27. A. K. Marnani, A. Bück, S. Antonyuk, B. van Wachem, D. Thévenin and J. Tomas, *Processes*, **7**, 439 (2019).
28. Y. Zhou, H. Ding, J. Zhu and Y. Shao, *Chem. Eng. J.*, **394**, 125039 (2020).